

1 **PSCA and MUC1 are targets of CAR T cells for treating NSCLC**

2 **PSCA and MUC1 in Non-small-cell Lung Cancer as Targets**
3 **of Chimeric Antigen Receptor T cells**

4 Xinru Wei^{1, 2, 3†}, Yunxin Lai^{1, 2, 3†}, Jin Li^{4†}, Le Qin^{1, 2, 3}, Youdi Xu^{1, 2, 3}, Rucong
5 Zhao^{1, 2, 3}, Baiheng Li^{1, 2, 3}, Simiao Lin^{1, 2, 3}, Suna Wang^{1, 2, 3}, Qiting Wu^{1, 2, 3}, Qiubin
6 Liang⁵, Muyun Peng⁶, Fenglei Yu⁶, Yangqiu Li⁷, Xuchao Zhang⁸, Yilong Wu⁸, Pentao
7 Liu⁹, Duanqing Pei^{1, 2}, Yao Yao^{1, 2, 3*}, Peng Li^{1, 2, 3*}

8
9 **Affiliations:**

10 ¹Key Laboratory of Regenerative Biology, South China Institute for Stem Cell
11 Biology and Regenerative Medicine, Guangzhou Institutes of Biomedicine and Health,
12 Chinese Academy of Sciences, Guangzhou, 510530, China;

13 ²Guangdong Provincial Key Laboratory of Stem Cell and Regenerative Medicine,
14 South China Institute for Stem Cell Biology and Regenerative Medicine, Guangzhou
15 Institutes of Biomedicine and Health, Chinese Academy of Sciences, Guangzhou,
16 510530, China;

17 ³State Key Laboratory of Respiratory Disease, Guangzhou Institutes of Biomedicine
18 and Health, Chinese Academy of Sciences, Guangzhou, 510530, China;

19 ⁴State Key Laboratory of Respiratory Disease, The First Affiliate Hospital of
20 Guangzhou Medical University, Guangzhou, 510500, China;

21 ⁵Guangdong Zhaotai InVivo Biomedicine Co. Ltd, Guangzhou, 510000, China;

22 ⁶Department of Thoracic Oncology, The Second Xiangya Hospital of Central South
23 University, Changsha, 410000, China;

24 ⁷Institute of Hematology, Medical College, Jinan University, Guangzhou, 510632,
25 China;

26 ⁸Guangdong Lung Cancer Institute, Medical Research Center, Guangdong General
27 Hospital, Guangdong Academy of Medical Sciences, Guangzhou, China;

28 ⁹Wellcome Trust Sanger Institute, Hinxton, Cambridge CB10 1HH, England, UK.

29
30 **Footnotes:** † indicates co-first authorship.

31 * **Correspondence:** Peng Li, PhD, Guangzhou Institutes of Biomedicine and Health,
32 Chinese Academy of Sciences, 190 Kaiyuan Avenue, Science Park, Guangzhou,
33 Guangdong, 510530, China; phone: +86-20-32093613; fax: +86-20-32093613, email:
34 li_peng@gibh.ac.cn; Yao Yao, Guangzhou Institutes of Biomedicine and Health,
35 Chinese Academy of Sciences, 190 Kaiyuan Avenue, Science Park, Guangzhou,
36 Guangdong, 510530, China; email: yao_yao@gibh.ac.cn.

Abstract

In recent years, immunotherapies, such as those involving chimeric antigen receptor (CAR) T cells, have become increasingly promising approaches to non-small-cell lung cancer (NSCLC) treatment. In this study, we explored the anti-tumor potential of prostate stem cell antigen (PSCA)-redirected CAR T and mucin 1 (MUC1)-redirected CAR T cells in tumor models of NSCLC. First, we generated patient-derived xenograft (PDX) mouse models of human NSCLC that maintained the antigenic profiles of primary tumors. Next, we demonstrated the expression of PSCA and MUC1 in NSCLC, followed by the generation and confirmation of the specificity and efficacy of PSCA- and MUC1-targeting CAR T cells against NSCLC cell lines in vitro. Finally, we demonstrated that PSCA-targeting CAR T cells could efficiently suppress NSCLC tumor growth in PDX mice and synergistically eliminate PSCA⁺MUC1⁺ tumors when combined with MUC1-targeting CAR T cells. Taken together, our studies demonstrate that PSCA and MUC1 are both promising CAR T cell targets in NSCLC and that the combinatorial targeting of these antigens could further enhance the anti-tumor efficacy of CAR T cells.

Key words: Non-small-cell lung cancer, Patient-derived xenograft, CAR T, PSCA, MUC1

1 Introduction

2 Globally, lung cancer is the greatest killer among all cancers^{1,2}, and
3 non-small-cell lung cancer (NSCLC) accounts for approximately 85% of all cases of
4 lung cancer^{3,4}. Current therapeutic strategies, including surgery, radiation and
5 chemotherapy, have not yielded significant survival benefits. Tyrosine kinase
6 inhibitors (TKIs) targeting EGFR and ALK have been widely used to treat NSCLC,
7 but frequent resistance to these drugs develops due to acquired mutations of EGFR⁵⁻⁷
8 and of ALK⁸. Furthermore, recently introduced CTLA4, PD-1 and PD-L1 immune
9 checkpoint inhibitors have had no⁹ or only moderate effects on NSCLC¹⁰⁻¹³. Therefore,
10 novel treatment regimens are still needed.

11 Chimeric antigen receptor (CAR) T cells that target CD19 have generated
12 exciting results in leukemia and lymphoma¹⁴⁻¹⁶. However, the broad applicability of
13 these cells for solid cancer is limited by the paucity of truly tumor-specific target
14 antigens. Additionally, the heterogeneity of tumor-associated antigens (TAAs) in solid
15 cancers complicates CAR T cell therapies, as the targets may differ among various
16 cancers and even patients of a same cancer. Therefore, it is important to define the
17 TAA profile of a solid cancer before using TAA-oriented personalized CAR T cell
18 immunotherapies.

19 Few CAR T cell antigens have been targeted to treat NSCLC. Glypican-3 was
20 recently reported as a promising target for lung squamous cell carcinoma¹⁷. In a phase
21 I clinical trial of anti-epidermal growth factor receptor (EGFR) CAR T cells for lung
22 cancer, only 2 of 11 patients achieved partial responses¹⁸. The expression of MUC1, a

1 transmembrane glycoprotein, is aberrantly upregulated in many types of cancer,
2 including NSCLC¹⁹. A trial of MUC1-targeting CAR T cells is currently recruiting
3 patients with four types of solid cancers, including NSCLC (ClinicalTrials.gov
4 Identifier: NCT02587689). Hence, MUC1 is a promising CAR T cell target in
5 NSCLC.

6 Prostate stem cell antigen (PSCA) is a glycosylphosphoinositol-anchored cell
7 surface antigen²⁰ that is overexpressed mainly in prostate cancer²¹, although its
8 expression has also been reported in other tumors such as gallbladder
9 adenocarcinoma²² and gastric cancer²³. Surprisingly, PSCA is frequently
10 overexpressed in NSCLC²⁰, although this requires confirmation. Antibody-based,
11 PSCA-targeted therapies, as well as a peptide vaccine, have been explored for the
12 treatment of prostate cancer²⁴⁻²⁸. Furthermore, PSCA-targeting CAR T cells have been
13 used to treat pancreatic cancer in humanized mice²⁹, and clinical trials of anti-PSCA
14 CAR T cells for the treatment of prostate, bladder and pancreatic cancers are ongoing
15 (ClinicalTrials.gov Identifier, NCT02092948 and NCT02744287). It remains
16 unknown, however, whether anti-PSCA CAR T cells could be used to treat NSCLC.

17 Patient-derived xenograft (PDX) models have been widely used in translational
18 cancer research³⁰, which faithfully resemble the original tumors from which they were
19 developed and this similarity is maintained across passages³¹. In this study, we
20 generated a PDX model of NSCLC in which we detected strong histological
21 expression of PSCA and weak expression of MUC1. We subsequently proved the
22 capacities of PSCA- and MUC1-targeted CAR T cells to recognize and kill NSCLC

cells expressing the respective target antigens. Finally, we observed enhanced efficacy of a combination of both PSCA- and MUC1-targeted CAR T cells against double-positive NSCLC samples. Our results suggest that PSCA and MUC1 are NSCLC-specific targets of CAR T cells and indicate that combinatorial antigen targeting could enhance the anti-tumor efficacy of these cells.

Results

1. PDX models retained molecular phenotype of NSCLC cells

Using TALEN-mediated gene targeting, we previously generated a NOD-SCID-IL2R $\gamma^{-/-}$ strain (NSI) of mice capable of engrafting and modeling human hematopoietic cells³². Here, we generated human NSCLC PDX mice by subcutaneously or intravenously implanting dissected primary tumor masses or cell suspensions that could be serially transplanted and engrafted in NSI mice.

Immunohistochemistry results showed that HLA⁺NSCLC cells from a patient (patient P2) that had been engrafted in the lungs of NSI mice expressed E-cadherin, but not vimentin, during both the first and second passages after transplantation (Fig. 1A).

Moreover, NSCLC cells from third passage of another patient (patient P1) metastasized from the initial subcutaneous implants to the livers and spleens of NSI mice, and tumor cells from all locations unanimously expressed vimentin but not E-cadherin (Fig. 1B). Therefore, PDX models of NSCLC retained the molecular phenotypes of NSCLC cells across different passages, as well as in different organs of metastasis.

2. Frequent expression of PSCA in NSCLC

NSCLC samples from 8 patients were successfully engrafted in NSI mice to generate PDX models (Table 1). We subsequently harvested the tumors and evaluated the expression of PSCA and MUC1. Although the latter is frequently overexpressed in NSCLC¹⁹, only 2 of the 8 patients in our study expressed this antigen; in contrast, 7 patients, including 2 patients who expressed MUC1, expressed PSCA (Fig. 2). Collectively, our results demonstrate the frequent expression of PSCA in human NSCLC cells, consistent with a previous report²⁰. The co-expression of PSCA and MUC1 in patients with NSCLC prompted an attempt to evaluate the efficacy of combination CAR T cells for dual antigen targeting in our PDX models.

3. Generation of CAR T cells targeting PSCA and MUC1

To redirect T lymphocytes to PSCA and MUC1, we used a second-generation PSCA-specific CAR and MUC1-specific CAR, which respectively consisted of the single-chain variable fragments (scFvs) derived from the humanized 1G8 anti-PSCA antibody³³ and anti-MUC1 HMFG2 monoclonal antibody³⁴, and signaling domains from the costimulatory molecule CD28 and the CD3 ζ (Fig. 3A). Lentiviral vectors encoding green fluorescent protein (GFP; negative control), CAR-PSCA and CAR-MUC1 were transfected into pre-activated human T cells to generate GFP T, CAR-PSCA T and CAR-MUC1 T cells, respectively. Transduction efficiencies were measured as the percentages of GFP⁺ cells (Fig. 3B). We used reverse transcription

1 polymerase chain reaction (PCR) analyses of the scFv sequences to further confirm
2 the expression of anti-PSCA CAR and anti-MUC1 CAR in T cells (Fig. 3C).

3

4 **4. CAR-PSCA T cells and CAR-MUC1 T cells specifically targeted PSCA⁺ and** 5 **MUC1⁺ lung cancer cells, respectively, in vitro**

6 We evaluated the specificity and efficacy of CAR-PSCA T cells against lung
7 cancer cell lines in vitro. First, in a PSCA expression analysis of three lung cancer cell
8 lines, A549, H23 and H460, only A549 cells were found to strongly express PSCA
9 (Fig. 4A). Immunohistochemistry analyses also consistently detected PSCA in A549
10 cells (Fig. 2). A luciferase-based in vitro killing assay demonstrated that CAR-PSCA
11 T cells specifically killed A549GL and H23-PSCA-GL cells (Fig. 4B). Enzyme-linked
12 immunosorbent assay (ELISA) results showed the PSCA-specific induction of IL-2
13 and IFN- γ production in supernatants from the killing assay (Fig. 4C). Taken together,
14 these findings indicate that CAR-PSCA T cells can recognize and kill PSCA⁺ cells in
15 vitro. We also confirmed the specificity and efficacy of CAR-MUC1 T cells. Like
16 PSCA, MUC1 was only detected on A549 cells, but not H23 and H460 cells (Fig. 4D).
17 CAR-MUC1 T cells killed A549GL and H23-MUC1-GL cells, but not H460GL or
18 H23GL cells, in vitro (Fig. 4E). We additionally observed MUC1-specific induction
19 of IL-2 and IFN- γ production in culture supernatants (Fig. 4F). Next, A549, H460,
20 H23 and H23-PSCA cells were transduced with a lentiviral vector expressing GFP
21 and luciferase (Fig. 4G), and H23-PSCA-GL and H23-MUC1-GL cells were

1 generating by transducing lentiviral vectors encoding PSCA and MUC1 into H23GL
2 cells (Fig. 4H).

3

4 **5. CAR-PSCA T cells were efficacious against PSCA⁺NSCLC in PDX mice**

5 We used a PDX model generated from the PSCA⁺, MUC1⁻ tumor of one patient
6 (patient P2) to further confirm the efficacy of CAR-PSCA T cells against NSCLC (Fig.
7 5A). Briefly, dissected tumor masses (~2 mm × 2 mm) were subcutaneously
8 transplanted in NSI mice to generate PDX mice, which subsequently received two
9 infusions of T cells (Fig. 5B); the tumors were calibrated until day 40. NSCLC tumor
10 mass growth was significantly suppressed by CAR-PSCA T cells, but not by
11 CAR-MUC1 T cells (Fig. 5C). On day 40, the smallest tumors were those in mice
12 treated with CAR-PSCA T cells (Fig. 5D), and tumors treated with CAR-PSCA T
13 cells had much lower weights than those left untreated or treated with GFP T cells
14 (Fig. 5E); however, no significant difference was found when CAR-MUC1 T cells
15 were used, further suggesting that our CAR T cells recognized and killed NSCLC
16 PDX tumors in an antigen-dependent manner. These results prove the efficacy of
17 CAR-PSCA T cells against PSCA⁺ NSCLC in PDX mice.

18

19 **6. CAR-PSCA T and CAR-MUC1 T cells synergistically inhibited NSCLC** 20 **growth in PDX mice**

21 We next evaluated the efficacy of a combination of CAR-PSCA T and
22 CAR-MUC1 T cells in a NSCLC PDX model generated from another patient (patient

P8) whose tumor expressed both PSCA and MUC1 (Fig. 5A). PDX mice were untreated (blank) or treated with identical numbers of GFP T, CAR-PSCA T, CAR-MUC1 T, or a 1:1 mix of CAR-PSCA T CAR-MUC1 T cells (Fig. 5F). Tumor growth was dramatically inhibited by CAR-PSCA T cells, CAR-MUC1 T cells and combined T cells (Fig. 5G-H). Furthermore, the tumor weights in mice treated with combined CAR T cells were significantly less than the weights in mice treated with a single type of CAR T cells (Fig. 5J-K). Collectively, the combination of CAR-PSCA and CAR-MUC1 T cells exhibited superior efficacy against NSCLC, compared with each cell type alone.

Discussion

The treatment of a majority of patients with solid cancers would require the development of genetically redirected T cells that target private somatic mutations, or neoantigens³⁵. However, this is an arduous task, given the heterogeneity of the mutational landscape within a tumor mass and between metastases. Despite the paucity of tumor-specific antigens shared across various types of solid cancers and among patients within one type of cancer, the TAAs of a single specific cancer are much less heterogeneous than neoantigens. Therefore, CAR T cell immunotherapy remains important during the development of neoantigen targeting techniques.

Although numerous TAAs have been detected in NSCLC³⁶, few have been targeted by CAR T cells^{37,38}. The use of these few non-cancer-specific antigens, which include FAP³⁹, EGFR⁴⁰, mesothelin⁴¹ and glypican-3¹⁷, has led to poor or undefined

therapeutic outcomes in patients. It is therefore important to broaden the NSCLC-specific targets of CAR T cells. PSCA-targeting CAR T cells have been developed^{29,42,43} and are ready for use in clinical trials of safety in patients with prostate, bladder and pancreatic cancers (ClinicalTrials.gov Identifier: NCT02092948 and NCT02744287). Additionally, a trial of MUC1-targeting CAR T cells is currently recruiting patients for NSCLC (ClinicalTrials.gov Identifier: NCT02587689). In this study, we frequently detected PSCA and MUC1 expression in NSCLC cells and thereby demonstrated the usefulness of anti-PSCA and anti-MUC1 CAR T cells.

Dual targeting of erbB2 and MUC1 by T cells expressing both CARs has been reported to deliver complimentary signals, enhance CAR T cell proliferation, but reduce IL-2 production⁴⁴. Combinatorial antigen recognition of PSCA and PSMA by a CAR that provides suboptimal activation and a chimeric costimulatory receptor (CCR) respectively has been reported to improve specificity and reduce off-target effects⁴². This strategy requires two types of chimeric receptors expressing on T cells together. In this study, we tested dual targeting of PSCA and MUC1 by mixed CAR T cells targeting either PSCA or MUC1 in NSCLC PDX models. Cancerous cells within a tumor mass may not unanimously express a single specific antigen, and even the PSCA⁺MUC1⁺ samples in our study might contain single positive cancerous cells, therefore, a CAR T cell-based combinatorial targeting strategy may broaden the populations of targeted cancerous cells.

Although the CAR-PSCA and CAR-MUC1 T cells used in our study caused considerable reductions in tumor sizes, they could not completely eradicate NSCLC in

PDX mice. This result could be attributed to the poor survival of CAR T cells in the immunosuppressive PDX tumor microenvironment. Strategies to improve the survival and infiltrating capacities of CAR T cells, such as optimized co-stimulation⁴⁵⁻⁴⁷ and cytokine co-expression⁴⁷⁻⁵¹, are worthy of exploration for all CAR T cells in solid tumors.

Overall, we have demonstrated that because PSCA and MUC1 are both rational targets in NSCLC, PSCA- and MUC1-targeting CAR T cells might comprise novel therapeutic agents for patients with NSCLC. Our results also suggest that a mixture of CAR T cells with different specificities could target simultaneously expressed tumor antigens and lead to better therapeutic outcomes.

Materials and Methods

Vector Design

To generate CAR-PSCA and CAR-MUC1 lentiviral vectors, scFvs derived from the humanized 1G8 anti-PSCA antibody³³ and anti-MUC1 HMFG2 monoclonal antibody³⁴ were codon optimized and synthesized by Genscript (Piscataway, NJ, USA). These scFvs were cloned into a CAR-encoding vector backbone comprising the CD8a leader sequence, human IgD hinge, portions of the CD28 transmembrane domains and the CD28 and CD3 ζ endodomains within the second-generation lentiviral vector pWPXLd. The amino acid (aa) sequences of the CARs were CD8a leader (aa 1-21), scFv, IgD hinge (aa 187-289), CD28 (aa 153-220), CD3 ζ (aa 52-163).

1 **Lentivirus production and transduction of primary human T cells**

2 Lentivirus particles were produced in HEK-293T cells via polyethyleneimine
3 (Sigma-Aldrich, St Louis, MO, USA) transfection. The pWPXLd-based lentiviral
4 plasmid and two packaging plasmids, psPAX2 and pMD.2G, were co-transduced into
5 HEK-293T cells. Lentivirus-containing supernatants were harvested at 48 and 72
6 hours post-transduction and filtered through a 0.45-um filter. Peripheral blood
7 mononuclear cells (PBMCs) were isolated from the buffy coats of healthy donors
8 using Lymphoprep (Fresenius Kabi Norge, AS, Berg i Østfold, Norway). T cells were
9 negatively selected from PBMCs using a MACS Pan T Cell Isolation Kit (Miltenyi
10 Biotec, Bergish Gladbach, Germany) and activated using microbeads coated with
11 anti-human CD3, anti-human CD2 and anti-human CD28 antibodies (Miltenyi Biotec)
12 at a 3:1 bead:cell ratio for 3 days in RPMI-1640 supplemented with 10% fetal bovine
13 serum (FBS), 10 mM HEPES, 2 mM glutamine and 1% penicillin/streptomycin. On
14 day 3 post-activation, T cells were transfected with CAR lentiviral supernatants in the
15 presence of 8 µg/ml polybrene (Sigma). Twelve hours post-transfection, T cells were
16 cultured in fresh media containing IL-2 (300 U/mL); subsequently, fresh media was
17 added every 2–3 days to maintain cell density within the range of $0.5\text{--}1 \times 10^6/\text{mL}$.
18 Healthy PBMC donors and all patients who provided primary patient specimens gave
19 informed consent to the use of their samples for research purposes, and all procedures
20 were approved by the Research Ethics Board of the Guangzhou Institutes of
21 Biomedicine and Health (GIBH).

22 **Cells and culture conditions**

HEK-293T cells were maintained in Dulbecco's modified Eagle's medium (Gibco, Grand Island, NY, USA). A549 (human lung adenocarcinoma), H23 (human lung adenocarcinoma), and H460 (human large cell lung cancer) cell lines were obtained from ATCC (Manassas, VA, USA) and maintained in RPMI-1640. Luciferase-GFP expressing cell lines (A549GL, H23GL and H460GL) were generated through transfection of the parental cell line with a lentiviral supernatant containing luciferase-2A-GFP and were sorted for GFP expression on a FACS AriaTM cell sorter (BD Biosciences, San Jose, CA, USA). H23-PSCA-GL or H23-MUC1-GL cells were generated by transfecting H23 cells with lentiviral supernatant. DMEM and RPMI-1640 media were supplemented with 10% heat-inactivated FBS (Gibco/Life Technologies), 10 mM HEPES, 2 mM glutamine (Gibco/Life Technologies) and 1% penicillin/streptomycin. All cells were cultured at 37 °C in an atmosphere of 5% carbon dioxide.

Flow cytometry

All samples were analyzed using an LSR Fortessa or C6 flow cytometer (BD Biosciences), and data were analyzed using FlowJo software (FlowJo, LLC, Ashland, OR, USA). The following antibodies were used: PSCA (clone 7F5) from Santa Cruz Biotechnology (Dallas, TX, USA) and anti-human CD227 (MUC-1, clone 16A⁵²) from Biolegend (San Diego, CA, USA). The clone 16A binds to glycopeptide RPAPGS(GalNAc)TAPPAHG of MUC1 (MUC1-Tn) with high affinity⁵². The scFv of HMFG2 (used to engineer the CAR) can recognize a range of tumor-associated MUC1 glycoforms, such as Tn, STn, T and ST (binds to MUC1-Tn and MUC1-STn

with higher affinity). HMFG2 has the broadest capacity for strong binding to tumor-associated MUC1 glycoforms³⁴. So the CAR-MUC1 T cells we generated can recognize the 16A positively stained cells.

In vitro tumor killing assays and cytokine release assays

A549GL, H23GL, H23-PSCA-GL or H23-MUC1-GL target cells were incubated with GFP T, CAR-PSCA T or CAR-MUC1 T cells at the indicated ratios in triplicate wells of U-bottomed 96-well plates. Supernatants were collected from wells with E:T ratios of 1:1 and subjected to an analysis of IL-2 and IFN- γ concentrations using ELISA kits (eBioscience, San Diego, CA, USA). Cells were treated with 100 μ l/well of the luciferase substrate D-luciferin (potassium salt, 150 μ g/ml; Cayman Chemical, Ann Arbor, MI, USA), and target cell viability was monitored using a microplate reader at a 450-nm excitation wavelength. Background luminescence was negligible (<1% of the signal from wells containing only target cells); therefore, the viability percentage (%) was equal to the experimental signal/maximal signal \times 100, and the killing percentage was equal to 100 - viability percentage.

PDX models for CAR T cell treatment

We used 6–8-week-old NSI mice according to protocols approved by the Institutional Animal Care and Use Committee of GIBH. All mice were maintained in specific pathogen-free (SPF)-grade cages and provided with autoclaved food and water. Surgical tumor samples were obtained from the Sun Yat-Sen University Cancer Center (Guangzhou, China) with informed consent of the patients; tumors were cut into 2 mm \times 2 mm pieces and directly transplanted subcutaneously without matrigel

1 or other additives into 3–6 immunodeficient NSI mice within a 30-min period.
 2 Tumors that reached an approximate size $<1000 \text{ mm}^3$ were removed and passaged to
 3 other NSI mice. On days 7 and 10, according to the doses used in other reports^{53,54}, $5 \times$
 4 10^6 total T cells were injected through the tail vein into each NSCLC-burdened NSI
 5 mouse. Tumors were measured every 4 days with a caliper to determine the
 6 subcutaneous growth rate. The tumor volume was calculated using the following
 7 equation: $(\text{length} \times \text{width}^2)/2$.

8 **Reverse Transcription (RT-PCR)**

9 mRNA was extracted from cells using RNeasy mini kit (Qiagen, Stockach, Germany)
 10 and reverse transcribed into cDNA using the PrimeScriptTM RT reagent Kit (Takara,
 11 Shiga, Japan). The following primers were used:

12 β -ACTIN forward: 5' AGAGCTACGAGCTGCCTGAC 3'

13 β -ACTIN reverse: 5' AGCACTGTGTTGGCGTACAG 3'

14 scFv of CAR-PSCA forward: 5' CTCTGTGGGGGATAGGGTCA 3'

15 scFv of CAR-PSCA reverse: 5' TCACAAGATTTGGGCTCGCT 3'

16 scFv of CAR-MUC1 forward: 5' TCGGTGGAGGAACCAAACTG 3'

17 scFv of CAR-MUC1 reverse: 5' CCTCCCTTTCACAGACTCCG 3'

18 **Immunohistochemistry**

19 Tumor tissue sections were fixed with 10% paraformaldehyde, embedded in paraffin,
 20 sectioned at a thickness of 4 μm , and stained using a standard hematoxylin and eosin
 21 technique. Paraffin sections were also immunostained with antibodies specific for
 22 E-cadherin (ZA0565), vimentin (ZA-0511), PSCA (ZA-0158), MUC1 (ZM-0391) and

1 HLA (Abcam, Cambridge, UK) overnight at 4 °C, followed by secondary staining with
2 secondary goat anti-mouse or goat anti-rabbit Ig (PV-9000) (ZSGB-BIO, Beijing,
3 China). Images of all sections were obtained with a microscope (DMI6000B; Leica
4 Microsystems, Wetzlar, Germany).

6 **Statistics**

7 Data are presented as means \pm standard errors of the means. Student's t-test was used
8 to determine the statistical significance of differences between samples, and a P value
9 <0.05 was considered to indicate a significant difference. All statistical analyses were
10 performed using Prism software, version 5.0 (GraphPad, Inc., San Diego, CA, USA).

12 **Acknowledgements**

13 This study was supported by the National Natural Science Foundation of China
14 (NSFC) - 81272329, 81522002, 81570156 and 81327801, Strategic Priority Research
15 Program of the Chinese Academy of Sciences (XDA01020310), the Natural Science
16 Fund for Distinguished Young Scholars of Guangdong Province (2014A030306028),
17 the Guangdong Provincial Applied Science and Technology Research &
18 Development Program (2016B020237006), the Guangdong Provincial Outstanding
19 Young Scholars Award (2014TQ01R068), the Guangdong Provincial Basic Research
20 Program (2015B020227003), the Guangdong Provincial Research and
21 Commercialization Program (2014B090901044), the Guangdong Province and
22 Chinese Academy of Sciences Joint Program for Research and Commercialization

1 Program (2013B091000010), the Guangzhou Basic Research Program
2 (201510010186), the MOST funding of the State Key Laboratory of Respiratory
3 Disease, and the National Basic Research Program of China (973 Program)
4 (2011CB504004 and 2010CB945500), the Frontier and key technology innovation
5 special grant from the Department of Science and Technology of Guangdong
6 province, (2014B020225005), the Guangzhou Science Technology and Innovation
7 Commission Project (201504010016).

8

9 **Conflict of Interest Statement**

10 The authors declare no competing financial interests.

11

12 **Authors and Contributors**

13 XW, YL, and JL contributed to the conception and design, collection and/or assembly
14 of data, data analysis and interpretation, and manuscript writing. LQ, YX, RZ, and QL
15 contributed to the provision of study material or patients, collection and/or assembly
16 of data. BL, SL, SW, and QW provided animal care and administrative supports. YY
17 and DP contributed to the conception and design and provided financial support. YY,
18 MP, FY, YL, XZ, YW, and PL contributed to the conception and design. XW and PL
19 contributed to the conception and design, data analysis and interpretation, manuscript
20 writing, and final approval of manuscript and provided financial support. All authors
21 read and approved the final manuscript.

22

References

1. Torre, L.A., *et al.* Global cancer statistics, 2012. *CA Cancer J Clin* **65**, 87-108 (2015).
2. Jemal, A., *et al.* Global cancer statistics. *CA Cancer J Clin* **61**, 69-90 (2011).
3. Qin, A., Coffey, D.G., Warren, E.H. & Ramnath, N. Mechanisms of immune evasion and current status of checkpoint inhibitors in non-small cell lung cancer. *Cancer Med* **5**, 2567-2578 (2016).
4. Zappa, C. & Mousa, S.A. Non-small cell lung cancer: current treatment and future advances. *Transl Lung Cancer Res* **5**, 288-300 (2016).
5. Thress, K.S., *et al.* Acquired EGFR C797S mutation mediates resistance to AZD9291 in non-small cell lung cancer harboring EGFR T790M. *Nat Med* **21**, 560-562 (2015).
6. Wang, S., Tsui, S.T., Liu, C., Song, Y. & Liu, D. EGFR C797S mutation mediates resistance to third-generation inhibitors in T790M-positive non-small cell lung cancer. *Journal of hematology & oncology* **9**, 59 (2016).
7. Wang, S., Cang, S. & Liu, D. Third-generation inhibitors targeting EGFR T790M mutation in advanced non-small cell lung cancer. *Journal of hematology & oncology* **9**, 34 (2016).
8. Wu, J., Savooji, J. & Liu, D. Second- and third-generation ALK inhibitors for non-small cell lung cancer. *Journal of hematology & oncology* **9**, 19 (2016).
9. Alexander, G.S., *et al.* Immune biomarkers of treatment failure for a patient on a phase I clinical trial of pembrolizumab plus radiotherapy. *Journal of hematology & oncology* **9**, 96 (2016).
10. Dang, T.O., Ogunniyi, A., Barbee, M.S. & Drilon, A. Pembrolizumab for the treatment of PD-L1 positive advanced or metastatic non-small cell lung cancer. *Expert review of anticancer therapy* **16**, 13-20 (2016).
11. Brahmer, J., *et al.* Nivolumab versus Docetaxel in Advanced Squamous-Cell Non-Small-Cell Lung Cancer. *The New England journal of medicine* **373**, 123-135 (2015).
12. Garon, E.B., *et al.* Pembrolizumab for the treatment of non-small-cell lung cancer. *The New England journal of medicine* **372**, 2018-2028 (2015).
13. Ma, W., Gilligan, B.M., Yuan, J. & Li, T. Current status and perspectives in translational biomarker research for PD-1/PD-L1 immune checkpoint blockade therapy. *Journal of hematology & oncology* **9**, 47 (2016).
14. Geyer, M.B. & Brentjens, R.J. Review: Current clinical applications of chimeric antigen receptor (CAR) modified T cells. *Cytotherapy* **18**, 1393-1409 (2016).
15. Park, J.H., Geyer, M.B. & Brentjens, R.J. CD19-targeted CAR T-cell therapeutics for hematologic malignancies: interpreting clinical outcomes to date. *Blood* **127**, 3312-3320 (2016).
16. Jackson, H.J., Rafiq, S. & Brentjens, R.J. Driving CAR T-cells forward. *Nature reviews. Clinical oncology* **13**, 370-383 (2016).
17. Li, K., *et al.* Adoptive immunotherapy using T lymphocytes redirected to glypican-3 for the treatment of lung squamous cell carcinoma. *Oncotarget* **7**, 2496-2507 (2016).
18. Feng, K., *et al.* Chimeric antigen receptor-modified T cells for the immunotherapy of patients with EGFR-expressing advanced relapsed/refractory non-small cell lung cancer. *Science China. Life sciences* **59**, 468-479 (2016).
19. Situ, D., *et al.* Expression and prognostic relevance of MUC1 in stage IB non-small cell lung

- 1 cancer. *Med Oncol* **28 Suppl 1**, S596-604 (2011).
- 2 20. Kawaguchi, T., *et al.* Clinical significance of prostate stem cell antigen expression in non-small
3 cell lung cancer. *Japanese journal of clinical oncology* **40**, 319-326 (2010).
- 4 21. Reiter, R.E., *et al.* Prostate stem cell antigen: a cell surface marker overexpressed in prostate
5 cancer. *Proceedings of the National Academy of Sciences of the United States of America* **95**,
6 1735-1740 (1998).
- 7 22. Zou, Q., Yang, L., Yang, Z., Huang, J. & Fu, X. PSCA and Oct-4 expression in the benign and
8 malignant lesions of gallbladder: implication for carcinogenesis, progression, and prognosis of
9 gallbladder adenocarcinoma. *BioMed research international* **2013**, 648420 (2013).
- 10 23. Zhao, X., Wang, F. & Hou, M. Expression of stem cell markers nanog and PSCA in gastric
11 cancer and its significance. *Oncology letters* **11**, 442-448 (2016).
- 12 24. [125I]Anti-prostate stem cell antigen antibody. (2004).
- 13 25. Ross, S., *et al.* Prostate stem cell antigen as therapy target: tissue expression and in vivo
14 efficacy of an immunoconjugate. *Cancer research* **62**, 2546-2553 (2002).
- 15 26. Matsueda, S., *et al.* Identification of new prostate stem cell antigen-derived peptides
16 immunogenic in HLA-A2(+) patients with hormone-refractory prostate cancer. *Cancer*
17 *immunology, immunotherapy : CII* **53**, 479-489 (2004).
- 18 27. Matsueda, S., *et al.* A prostate stem cell antigen-derived peptide immunogenic in HLA-A24-
19 prostate cancer patients. *The Prostate* **60**, 205-213 (2004).
- 20 28. Gu, Z., Yamashiro, J., Kono, E. & Reiter, R.E. Anti-prostate stem cell antigen monoclonal
21 antibody 1G8 induces cell death in vitro and inhibits tumor growth in vivo via a
22 Fc-independent mechanism. *Cancer research* **65**, 9495-9500 (2005).
- 23 29. Abate-Daga, D., *et al.* A novel chimeric antigen receptor against prostate stem cell antigen
24 mediates tumor destruction in a humanized mouse model of pancreatic cancer. *Human gene*
25 *therapy* **25**, 1003-1012 (2014).
- 26 30. Hidalgo, M., *et al.* Patient-derived xenograft models: an emerging platform for translational
27 cancer research. *Cancer Discov* **4**, 998-1013 (2014).
- 28 31. Dong, R., *et al.* Histologic and molecular analysis of patient derived xenografts of high-grade
29 serous ovarian carcinoma. *Journal of hematology & oncology* **9**, 92 (2016).
- 30 32. Ye, W., *et al.* Quantitative evaluation of the immunodeficiency of a mouse strain by tumor
31 engraftments. *Journal of hematology & oncology* **8**, 59 (2015).
- 32 33. Olafsen, T., *et al.* Targeting, imaging, and therapy using a humanized antiprostate stem cell
33 antigen (PSCA) antibody. *J Immunother* **30**, 396-405 (2007).
- 34 34. Wilkie, S., *et al.* Retargeting of Human T Cells to Tumor-Associated MUC1: The Evolution of a
35 Chimeric Antigen Receptor. *The Journal of Immunology* **180**, 4901-4909 (2008).
- 36 35. Klebanoff, C.A., Rosenberg, S.A. & Restifo, N.P. Prospects for gene-engineered T cell
37 immunotherapy for solid cancers. *Nat Med* **22**, 26-36 (2016).
- 38 36. Djureinovic, D., *et al.* Profiling cancer testis antigens in non-small-cell lung cancer. *JCI insight* **1**,
39 e86837 (2016).
- 40 37. Beatty, G.L. & O'Hara, M. Chimeric antigen receptor-modified T cells for the treatment of
41 solid tumors: Defining the challenges and next steps. *Pharmacology & therapeutics* **166**,
42 30-39 (2016).
- 43 38. Di, S. & Li, Z. Treatment of solid tumors with chimeric antigen receptor-engineered T cells:
44 current status and future prospects. *Science China. Life sciences* **59**, 360-369 (2016).

- 1 39. Kakarla, S., *et al.* Antitumor effects of chimeric receptor engineered human T cells directed to
2 tumor stroma. *Molecular therapy : the journal of the American Society of Gene Therapy* **21**,
3 1611-1620 (2013).
- 4 40. Zhou, X., *et al.* Cellular immunotherapy for carcinoma using genetically modified
5 EGFR-specific T lymphocytes. *Neoplasia* **15**, 544-553 (2013).
- 6 41. Morello, A., Sadelain, M. & Adusumilli, P.S. Mesothelin-Targeted CARs: Driving T Cells to Solid
7 Tumors. *Cancer Discov* **6**, 133-146 (2016).
- 8 42. Kloss, C.C., Condomines, M., Cartellieri, M., Bachmann, M. & Sadelain, M. Combinatorial
9 antigen recognition with balanced signaling promotes selective tumor eradication by
10 engineered T cells. *Nature biotechnology* **31**, 71-75 (2013).
- 11 43. Hillerdal, V., Ramachandran, M., Leja, J. & Essand, M. Systemic treatment with
12 CAR-engineered T cells against PSCA delays subcutaneous tumor growth and prolongs
13 survival of mice. *BMC cancer* **14**, 30 (2014).
- 14 44. Wilkie, S., *et al.* Dual targeting of ErbB2 and MUC1 in breast cancer using chimeric antigen
15 receptors engineered to provide complementary signaling. *J Clin Immunol* **32**, 1059-1070
16 (2012).
- 17 45. Long, A.H., *et al.* 4-1BB costimulation ameliorates T cell exhaustion induced by tonic signaling
18 of chimeric antigen receptors. *Nat Med* **21**, 581-590 (2015).
- 19 46. Song, D.G., *et al.* CD27 costimulation augments the survival and antitumor activity of
20 redirected human T cells in vivo. *Blood* **119**, 696-706 (2012).
- 21 47. Hombach, A.A., Heiders, J., Foppe, M., Chmielewski, M. & Abken, H. OX40 costimulation by a
22 chimeric antigen receptor abrogates CD28 and IL-2 induced IL-10 secretion by redirected
23 CD4(+) T cells. *Oncoimmunology* **1**, 458-466 (2012).
- 24 48. Hoyos, V., *et al.* Engineering CD19-specific T lymphocytes with interleukin-15 and a suicide
25 gene to enhance their anti-lymphoma/leukemia effects and safety. *Leukemia* **24**, 1160-1170
26 (2010).
- 27 49. Perna, S.K., *et al.* Interleukin 15 provides relief to CTLs from regulatory T cell-mediated
28 inhibition: implications for adoptive T cell-based therapies for lymphoma. *Clinical cancer*
29 *research : an official journal of the American Association for Cancer Research* **19**, 106-117
30 (2013).
- 31 50. Perna, S.K., *et al.* Interleukin-7 mediates selective expansion of tumor-redirection cytotoxic T
32 lymphocytes (CTLs) without enhancement of regulatory T-cell inhibition. *Clinical cancer*
33 *research : an official journal of the American Association for Cancer Research* **20**, 131-139
34 (2014).
- 35 51. Markley, J.C. & Sadelain, M. IL-7 and IL-21 are superior to IL-2 and IL-15 in promoting human
36 T cell-mediated rejection of systemic lymphoma in immunodeficient mice. *Blood* **115**,
37 3508-3519 (2010).
- 38 52. Song, W., *et al.* MUC1 glycopeptide epitopes predicted by computational glycomics.
39 *International journal of oncology* **41**, 1977-1984 (2012).
- 40 53. O'Hear, C., Heiber, J.F., Schubert, I., Fey, G. & Geiger, T.L. Anti-CD33 chimeric antigen receptor
41 targeting of acute myeloid leukemia. *Haematologica* **100**, 336-344 (2015).
- 42 54. Qin, H., *et al.* Eradication of B-ALL using chimeric antigen receptor-expressing T cells targeting
43 the TSLPR oncoprotein. *Blood* **126**, 629-639 (2015).
- 44

Figure legends

Figure 1. Generation and molecular characterization of patient-derived

xenograft (PDX) models of non-small-cell lung cancer. (A) Hematoxylin and eosin

(H&E) staining and immunohistochemistry detection of human leukocyte antigen

(HLA), E-cadherin and vimentin in tumor sections from both the first and second

passages of PDX mice for patient P2 (see from figure 2). Although HLA⁺ cells from

PDX mice also expressed E-cadherin, cells from both passages were negative for

vimentin. (B) H&E staining and immunohistochemistry detection of HLA, E-cadherin

and vimentin in sections from liver, spleen and subcutaneous (s.c.) tissue. All sections

were from a single mouse among the third passage of PDX mice for patient P1 (see

from figure 2). Scale bar = 20 μ m.

Figure 2. Sections of tumors from eight patient-derived xenograft (PDX) models.

Representative images correspond to tumors derived from eight patients; all sections

were stained with hematoxylin and eosin (H&E) and antibodies against human

leukocyte antigen (HLA), PSCA and MUC1. The passage numbers of each PDX for

the patients were indicated. The negative controls (NC) are the liver tissues from a

same mouse of third passage of PDX for patient P3. Scale bar = 20 μ m. PSCA and

MUC1 detection results are also shown in Table 1.

Figure 3. Construction of anti-prostate stem cell antigen (PSCA) and anti-mucin

1 (MUC1) chimeric antigen receptor (CAR) T cells. (A) Structures of the genes

used for lentiviral transfection. GFP, control without CAR; CAR-PSCA, anti-PSCA

CAR; CAR-MUC1, anti-MUC1 CAR. (B) Representative flow cytometric analysis of

1 transfected T cells. (C) Reverse transcription-PCR detection of the following:
2 β -ACTIN in wild type (WT), CAR-PSCA and CAR-MUC1 T cells (left); anti-PSCA
3 scFv in WT and CAR-PSCA T cells and CAR-PSCA vector as a positive control
4 (middle) and anti-MUC1 scFv in WT and CAR-MUC1 T cells and CAR-MUC1
5 vector as a positive control (right).

6 **Figure 4. T cells expressing the prostate stem cell antigen (PSCA) or mucin 1**
7 **(MUC1) chimeric antigen receptor (CAR) specifically killed PSCA⁺ or MUC1⁺**

8 **lung cancer cell lines, respectively, in vitro.** (A) Flow cytometric analysis of PSCA
9 expression on A549, H23 and H460 cell lines. (B) Percentages of lung cancer line
10 cells killed by GFP T cells and CAR-PSCA T cells at the indicated effector (E): target

11 (T) ratios. The ratios were of the absolute number of CAR T cells vs target cells
12 (corrected for transduction efficiency). T cells were cocultured with A549GL,

13 H460GL, H23GL or H23-PSCA-GL cells for 18 h, and luciferase activities were
14 measured using a D-luciferin substrate. % of killing = % (total activities without T
15 cells – activities with T cells)/ total activities without T cells. Data were representative

16 of killing assays using T cells from three different donors. (C) Results of

17 enzyme-linked immunosorbent assays (ELISAs) to detect IL-2 and IFN- γ in the

18 supernatants of cocultures at a E: T ratio of 1:1. (D) Flow cytometric analysis of

19 MUC1 expression on A549, H23 and H460 cell lines. (E) Percentages of lung cancer

20 line cells killed by GFP T cells and CAR-MUC1 T cells at the indicated E: T ratios. (F)

21 Results of ELISAs to detect IL-2 and IFN- γ in the supernatants of cocultures at a E: T

22 ratio of 1:1. Data were representative of killing assays using T cells from three

different donors. (G) Post-transfection GFP-Luciferase (GL) expression was detected in A549GL, H23GL and H460GL cell lines by flow cytometry. GFP served as a marker of luciferase expression. (H) Flow cytometric detection of PSCA (left) and MUC1 (right) in H23GL cells after lentiviral transduction. Error bars denote standard errors of the means, and groups were compared using the unpaired *t*-test. * *P* <0.05, ** *P* <0.01, *** *P* <0.001.

Figure 5. Prostate stem cell antigen chimeric antigen receptor (CAR-PSCA) expressing T cells inhibit the growth of non-small-cell lung cancer (NSCLC) and exhibit synergistic efficacy with mucin 1 CAR (CAR-MUC1) expressing T cells against NSCLC in patient-derived xenograft (PDX) models. (A) Diagram of the experiment with primary NSCLC tumors from patient P2 or P8 in NSI mice. Mice were inoculated subcutaneously with dissected tumor masses from patient P2 or P8 (2 mm × 2 mm), infused with 5×10^6 total T cells on days 7 and 10, and culled on day 40 for tumor analysis. B-E were results from the PDX model of patient P2. (B) T cells were analyzed for transfection efficiency before infusion into PDX mice of patient P2. (C) Tumor growth curves in groups treated with no T (n=3), GFP T (n=3), CAR-PSCA T (n=4) or CAR-MUC1 T (n=4) cells. (D) Tumors from mice treated with no T, GFP T, CAR-PSCA T or CAR-MUC1 T cells on day 40 are shown. One mouse from both the no T and GFP T groups died when tumors were small, which was not shown. (E) Comparison of the weights of tumors described in D. F-J were results from the PDX model of patient P8. (F) T cells were analyzed for transfection efficiency before infusion into PDX mice of patient P8. (G) Tumor growth curves in

1 groups treated with no T (n=3), GFP T (n=3), CAR-PSCA T (n=4), CAR-MUC1 T
2 (n=4), and combinatorial CAR T cells (n=4). (H) Tumors from different groups in G
3 on day 40 were shown. Also, both the no T and GFP T groups had one mouse died
4 when tumors were small. (I) Comparison of the weights of tumors in H. (J) Tumors
5 from CAR-PSCA T, CAR-MUC1 T and combinatorial groups were singled out for
6 comparison. Error bars denote standard errors of the means, and groups were
7 compared using the unpaired *t*-test. * $P < 0.05$, ** $P < 0.01$, *** $P < 0.001$.

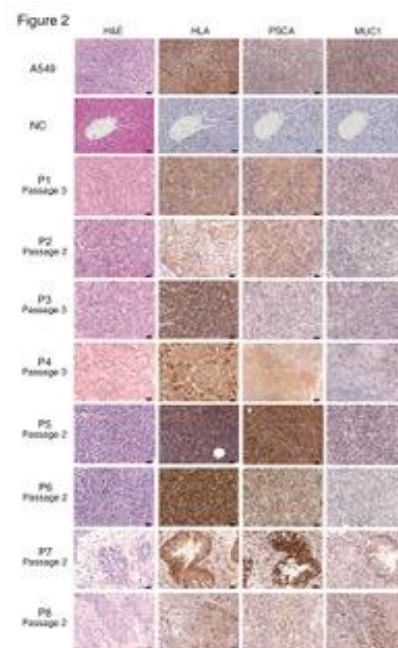
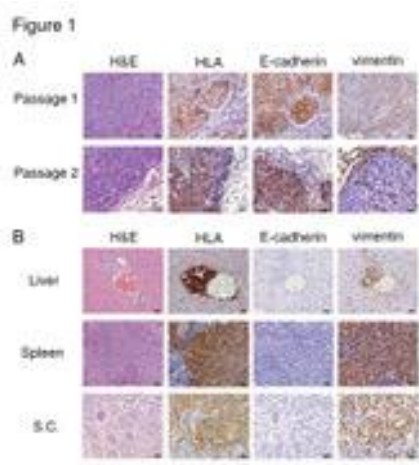




Table 1

Clinical information of the patients and characteristics of the corresponding PDX models

Patient	Gender	Age	Pathology	PSCA	MUC1	E-cadherin (primary/PDX)	Vimentin (primary/PDX)	Metastasis in PDX	Route of administration
P1	M	60	AC	+	-	-/-	+/+	Yes	SC
P2	M	69	AC	+	-	+/+	-/-	No	IV
P3	M	65	AC	-	-	-/-	+/+	Yes	SC
P4	M	67	LCC	+	-	+/+	-/-	No	SC
P5	M	51	AC	+	-	ND	ND	No	SC
P6	F	57	AC	+	-	ND	ND	Yes	SC
P7	F	72	SCC	+	+	ND	ND	No	SC
P8	F	58	SCC	+	+	ND	ND	No	SC

M, male; F, female, AC, adenocarcinoma; LCC, large cell carcinoma; SCC, squamous cell carcinoma; +, expression; -, no expression; ND, not detected; SC, subcutaneous; IV, intravenous.